Influence of vibration on mechanical polishing micro-structured surface using discrete element method

Guilian Wang, Bingrui Lv and Li Liu

Tianjin Key Laboratory for Advanced Mechatronic System Design and Intelligent Control,
School of Mechanical Engineering
and
National Demonstration Center for Experimental Mechanical and Electrical Engineering Education,
Tianjin University of Technology,
Tianjin 300384, China
Email: wangguilian94@163.com
Email: 15122160890@163.com
Email: 632381465@qq.com

Bin Liu

Tianjin Laboratory of Control Theory and Applications in Complicated System,
Tianjin 300384, China
and
School of Electrical and Electronic Engineering,
Tianjin University of Technology,
Tianjin 300384, China
Email: lbin83@126.com

Haibo Zhou*

Tianjin Key Laboratory for Advanced Mechatronic System Design and Intelligent Control,
School of Mechanical Engineering
and
National Demonstration Center for Experimental Mechanical and Electrical Engineering Education,
Tianjin University of Technology,
Tianjin 300384, China
Email: haibo_zhou@163.com
*Corresponding author

Abstract: A model using discrete element method (DEM) was conducted to simulate vibration assisted mechanical polishing micro-structured surface process by particle flow code in three dimensions (PFC^{3D}). The effect laws of vibration frequency and amplitude on abrasive grains and polishing force were

researched in detail according to the simulation results. The effects of vibration on the particles average motion velocity in one fluid cell were researched, and the simulation results show that average velocity increases with increase of vibration frequency and amplitude on the whole. The effects of vibration on the unbalanced force acting on the workpiece surface were quantified at first. The changes of average unbalanced force obviously increase for low feed rate with increase of frequency and increase approximately linearly with increase of amplitude. It is concluded that vibration with high frequency and great amplitude can significantly increase machining efficiency and improve surface quality in micro-structured surface polishing.

Keywords: polishing; vibration; micro-structured surface; discrete element method; DEM.

Reference to this paper should be made as follows: Wang, G., Lv, B., Liu, L., Liu, B. and Zhou, H. (2020) 'Influence of vibration on mechanical polishing micro-structured surface using discrete element method', *Int. J. Machining and Machinability of Materials*, Vol. 22, No. 1, pp.24–46.

Biographical notes: Guilian Wang is an Associate Professor at the School of Mechanical Engineering, Tianjin University of Technology in China. Her research area is the intelligent precision manufacture.

Bingrui Lv is a graduate at the School of Mechanical Engineering, Tianjin University of Technology in China. His research area is the intelligent precision manufacture.

Li Liu is a Lecturer at the School of Mechanical Engineering, Tianjin University of Technology in China. His research area is the failure mechanism and optimal design of cutting tool.

Bin Liu is an Associate Professor at the School of Electrical and Electronic Engineering, Tianjin University of Technology in China. His research area is the instrument science and technology.

Haibo Zhou is a Professor at the School of Mechanical Engineering, Tianjin University of Technology in China. His research area is the intelligent robot technology.

1 Introduction

As micro-structured optical components are being widely used in many fields such as national defence astronautics, the technology of producing moulds for these components becomes more and more important. It is all known that the vibration assisted mechanical polishing micro-structured surface is a very complex material removal process and the obvious differences appear in its polishing efficiency and machining quality with the changes in vibration frequency and amplitude. The researchers have been explored material removal mechanism interacting with the solid-liquid coupling system containing abrasives and polishing liquid under different vibration efficiency by polishing experiments. In fact, the vibration on the state motion and cutting property of abrasives participating in cutting workpiece surface and the force acting on the workpiece have

some changes. However, these phenomena can't be observed due to the precision of apparatus at the present. With the help of simulation, involving the effects of vibration on it has important guiding significance for optimising processing parameters, increasing polishing efficiency and improving surface quality.

In existing researches on material removal mechanism of vibration assisted polishing (Yu et al., 2018), the effects of processing parameters such as polishing pressure (Yang et al., 2015; Han et al., 2015), vibration parameters (Song et al., 2016; Xu et al., 2011; Li et al., 2014a; Zhao et al., 2016; Mullany and Mainuddin, 2012; Maroju et al., 2017; Li et al., 2019) and shapes of abrasives (Liang et al., 2016; Zhu et al., 2016) on material removal rate (Guo and Suzuki, 2018; Wang et al., 2018) and surface roughness were usually researched by using theoretical and experimental methods, and polishing mechanism was analysed by means of microscopic characterisation (Belkhir et al., 2014; Cao et al., 2016; Salvatore et al., 2017; Li et al., 2012; Hreha and Hloch, 2013). At present, the mechanism of how the vibration parameters (frequency, amplitude) affect the polishing fluid pressure, distributions and movement characteristics of abrasives and other aspects are not well explained up to now, because these physics phenomena cannot be observed by using modern instruments. In recent years, researchers at home and abroad have committed to researching grinding (Liedke and Kuna, 2013; Iliescu et al., 2010; Xiu et al., 2007), polishing (Lin et al., 2006; Fan et al., 2007; Han and Gan, 2011; Eder et al., 2015; Agrawal et al., 2010; Sun et al., 2014; Huuki and Laakso, 2017), other machining processes (André et al., 2012, 2014; Li et al., 2014b; Ancio et al., 2018), friction and contacts of moving surface (Jerier and Molinari, 2012) by means of numerical simulation methods. Among these numerical simulation methods, discrete element method (DEM) originated from molecular dynamics was first proposed by Cundall in the 1970s. It is suitable for simulating discrete particles combinations' deformation and failure process on quasi-static or dynamic condition. Currently, the researches on polishing using the DEM are as follows:

In the polishing process respect: Han (2014) developed a discrete element model for polycrystalline Si_3N_4 ceramics to study the ceramics polishing process. The simulation results justified that the common critical depth of cut can't be used as the effective parameters for evaluating brittle to ductile transformation in the ceramic polishing process. Uhlmann et al. (2015) researched the drag finishing and modelled the movement of media and workpiece by using the DEM, which was used for determining local contact intensities on the workpiece surface and between particles. Jiang et al. (2015) presented a DEM methodology for simulating the grinding process of SiC ceramics. This model describes the relationship between the material removal, the initiation and propagation of cracks and the changes in grinding force of grinding process in quantity. The grinding process simulation of ceramic materials for different grinding parameters was finished by using this model. To investigate the material removal and surface topography formation in vibratory finishing, Uhlmann et al. (2014) developed a comprehensive process model combining the DEM with experimental results, where DEM is used to model the motion of the bulk of abrasive particles and its contacts with the workpiece.

In the workpiece surface respect: André et al. (2013) used the DEM to simulate brittle fracture in the indentation of a silica glass with a blunt indenter and presented a novel failure criterion based on an equivalent hydrostatic stress. Iordanoff et al. (2008) established a discrete element model to investigate sub-surface damage due to surface

polishing. It is shown how the mechanical properties (pressure), the abrasive properties (shape and quantity of abrasive particles) and the system properties (filtration) have an influence on the sub-surface properties at the end of the process. In order to subsurface mechanical damage during bound abrasive grinding of fused silica glass, Blaineau et al. (2015) established the grinding process interface model using a DEM and found a relation between the subsurface damage depth and the grinding forces normalised by the abrasive concentration. Tan et al. (2009) developed the polycrystalline SiC ceramics model to study the machining process of ceramics. Simulation results have clearly demonstrated rational trends of the correlations between microscopic damage on the finished surface and the cutting conditions.

In the abrasive grains respect: Fillot et al. (2007) established third body flowing model with a DEM in order to study the wear process of the adhesive particles by considering the detachment of particles, their flow in the contact and their ejection. Three-body abrasion is an important abrasive process in the surface polishing. Loresch and Riemer (2015) presented the rolling motion model of abrasive grain for three-body abrasion by splitting the integral removal volume under the polishing pad into the removal of single grains and distributing the total polishing force according to the interaction of individual grains with the workpiece material.

Previous studies have reported much valuable insights into material removal mechanisms of vibration assisted polishing micro-structured surface. From what has been discussed above, it can draw a conclusion that, by researching the surface generation mechanism, the subsurface damage, stress variation of polishing contact region, abrasive movement without fluid and wear, and other aspects of mechanical polishing process using the DEM, movement characteristics of abrasives in polishing region and the changes of stress at different moments have been gained. However, regarding simulation of vibration assisted mechanical polishing micro-structured surface, the researches on the action mechanism of vibration on abrasive grains motion cutting workpiece surface and the force acting on the workpiece surface have not been reported up to now, which has important significance for revealing the material removal mechanism. As a result, these aspects were researched in this study. Based on the DEM, a simulation of vibration assisted mechanical polishing micro-structured surface was performed to systematically study and analyse the functions of vibration at the interaction of solid and liquid in polishing.

2 Model descriptions

2.1 Vibration assisted polishing microstructure surface

Figure 1 shows the schematic diagram of vibration assisted mechanical polishing micro-structured surface, which consists of a rotating workpiece, a vibrating polishing tool and the polishing liquid containing the abrasive grains. The polishing tool applies a force against the workpiece surface and there is a constant pressure in contacting region between the workpiece and the tool according to the theory. The workpiece surface is micro-cut by the abrasive grains that have high speed and energy driven by rotating of workpiece and vibrating of polishing tool.

Figure 1 Vibration assisted mechanical polishing micro-structured surface (see online version for colours)

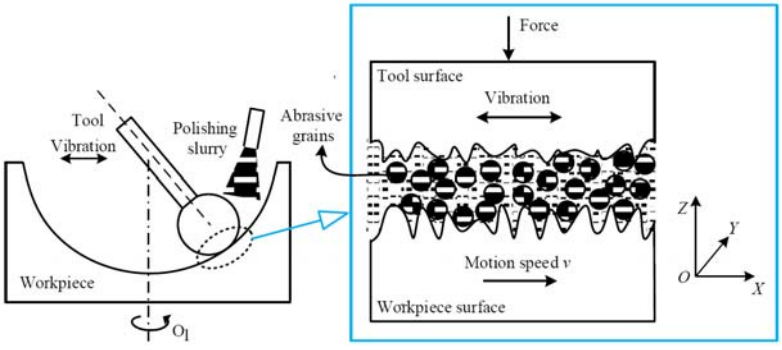

2.2 Modelling

In order to simplify the problem, the modelling objects are the following assumption:

1 the contact area of workpiece contacting with the tool is assumed to be a plane

2 the workpiece's rotational motion is replaced by the translation motion

3 the abrasives are assumed to be spherical

4 the particle radius is much smaller than the length of a single fluid element

5 the type of contact among particles is set as liner-elastic.

A micro structure in the contact area of workpiece and polishing tool is modelled and simulated. The contact area of the workpiece and the polishing tool is $4.39 * 10^{-8}$ m^2.The workpiece and the polishing tool are constructed by 'clump' in PFC^{3D}. The abrasives are represented by 'particles'. The polishing liquid is constructed by fluid calculation function in PFC^{3D} and represented by 'fluidcell'. The workpiece and polishing tool are constructed with clumps. A clump is a rigid body comprising of spheres. The spheres within a clump may overlap to any extent, and each clump behaves as a rigid body (with deformable boundaries) that will not break apart regardless of the forces acting upon it. The rough surfaces between the workpiece and the tool are represented by the surfaces of clumps comprising of spheres in order to simply the model, which are different from the reality to some extent, however, the focus of this study is the effects of vibration on the abrasives motion velocity and unbalanced force at the nanoscale rather than the effects of the material removal process of abrasives on workpiece surface topography. Gravity and buoyancy are not considered because the abrasives are suspended in the polishing liquid. The damping coefficient is set as 0.1. The steps are as follows:

1 Polishing tool: the polishing tool vibrates only in *x*-direction in this study. The material of polishing tool is polyurethane. It is constructed by a clump consisting of 32 particles whose radiuses is 30 μm, densities is 1,170 kg/m^3, normal stiffness is

$6 * 10^4$ N/m, tangential stiffness is $6 * 10^4$ N/m and friction coefficients is 0.2. The length, width and height of the clump are 405 μm, 187.3 μm and 60 μm respectively.

2 Workpiece: the material of workpiece is silicon carbide. It is constructed by a clump consisting of 200 particles whose radius is 30 μm, density is 3,200 kg/m^3, normal stiffness is $4.92 * 10^7$ N/m, tangential stiffness is $4.92 * 10^7$ N/m and friction coefficient is 0.12. The length, width and height of the clump are 1,026 μm, 216.5 μm and 60 respectively. The length of clump is enough for simulation in this study.

3 Abrasive grains: the material of abrasive grains is diamond. They consist of 500 particles whose radius are 0.25 μm, density is 3,500 kg/m^3, normal stiffness is $1.32 * 10^8$ N/m, tangential stiffness is $1.32 * 10^8$ N/m and friction coefficient is 0.08.

4 Applying force: at the beginning, *Z* coordinate of polishing tool is 62 μm. A force paralleling to along *Z* axial positive direction (0.03) is applied to the upper of the polishing tool, which makes the polishing tool move down and contact with the workpiece surface, as shown in Figure 2. In Figure 2, the direction and magnitude of the arrows represent the direction and magnitude of particles' velocities. It takes enough time for the model to get a stable condition where the value of particles' velocities is very small.

5 Polishing fluid: the polishing fluid is incompressible viscous fluid. The material of polishing liquid is water at room temperature. The density is 997.048 kg/m^3 and the viscosity is $0.8937 * 10^{-3}$ Pa * s. A fluidcell (length: 250 μm, width: 130 μm, height: 130 μm) is adopted to represented the polishing liquid. Fluid boundary conditions are applied at the outside of the fluidcell. Boundary condition 'press', fluid can flow across boundary portions, is applied at the around and the upper of the fuidcell. Boundary condition 'slip', fluid can't flow across boundary portions, is applied at the lower of the fuidcell.

6 Polishing model: when this system of tool, abrasive grains and workpiece (Figure 3) can get a stable condition after applying a force, fluidcell is added to the system, and then whole polishing model is completed, as shown in Figure 3.

Figure 2 Polishing tool moving down to contact with the workpiece (see online version for colours)

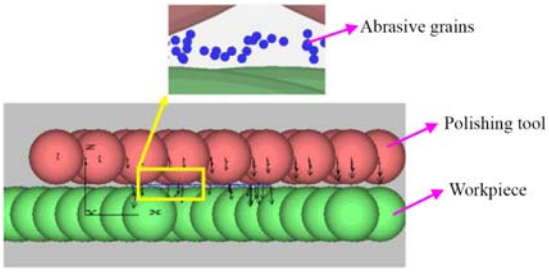

Figure 3 Three-dimensional polishing model (see online version for colours)

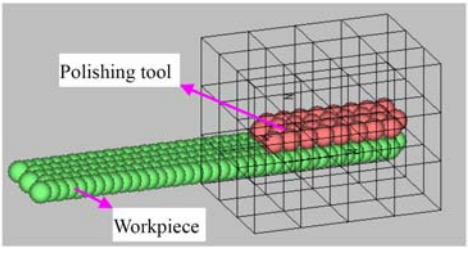

3 Simulation results and discussion

3.1 The effects of vibration on the particle velocity

In this study, the simulation parameters were chosen according to the references (Guo et al., 2012, 2013; Suzuki et al., 2006, 2010). The feed rates of workpiece are 3.52 m/s and 5.23 * 10^{-3} m/s respectively when vibration frequency rages are 7,000 Hz to 30,000 Hz. The polishing force is 30 mN and the vibration amplitude is 30 μm. Every simulation time is 2 * 10^{-4} s. During PFC^{3D} simulations, the velocities of all particles in *X*, *Y* and *Z*-direction in one fluidcell were all recorded respectively at every moment.

3.1.1 The effects of vibration frequency on the particle velocity

For all particles in one fluidcell at every moment, the magnitudes of their resultant velocities were calculated. The simulation results show that the particle velocity in the *X* direction is very high, however, that of *Y* is very low and that of *Z* is almost equal to zero, which is because of vibration direction paralleling to *X* axis. Figure 4 and Figure 5 show that *X*-direction velocity and whole motion velocity changes of abrasive grains at different vibration frequencies when feed rate is equal to 5.23 * 10^{-3} m/s, respectively. Figure 6 is the average velocity versus vibration frequency for two feed rates.

It can be seen from Figure 4 that the change of particles *X*-direction velocity is very rapid at the begin of polishing, the particles velocity goes into a stable stage after 2.5 * 10^{-5} s, all the change curves of velocity are similar to the sinusoidal curves and closely related to the vibration frequency. The feature similar to the sinusoidal curves is more obvious with increase of vibration frequency gradually. In the Figure 4, the *X*-direction average velocities of the particles are 0.3681 m/s, 0.2518 m/s, 0.6914 m/s, 1.1520 m/s respectively when vibration frequencies are 7,000 Hz, 10,000 Hz, 20,000 Hz and 30,000 Hz. In addition, Figure 5 shows the motion velocity of abrasive grains after entering the stable stage. For 7,000 Hz, the periodicity of velocity change is not very

obvious because the simulation time is just 0.0002 s. However, it can be seen from Figures 5(b), 5(c) and 5(d) that all the velocity change curves are also similar to the sinusoidal curves, with increase of vibration frequency, the feature similar to the sinusoidal curves is also more evident and the maximum velocity also increases. It is concluded from these analyses that the direction of particle motion is closely related to the vibration direction and the vibration frequency has important effects on the abrasives' active degree.

Figure 6 shows the changes of particles average velocity with increase of vibration frequencies when feed rates are $5.23 * 10^{-3}$ m/s and 3.52 m/s respectively. As shown Figure 6, the velocity of abrasive grains increases with increase of vibration frequency on the whole whatever the feed rate of workpiece is high or low. It is concluded that vibration plays a major role in abrasive grain motion, indicating that vibration assisted polishing can increase material removal rate and decrease surface roughness of workpiece. According to the motion theory, motion speed of abrasive grain is provided by interaction of workpiece movement and polishing tool vibration. To be specific, the vibration plays a major role especially when the feed rate of workpiece is low, and the vibration and the workpiece movement common play a major role when the feed rate of workpiece is high. However, it can be found by comparing two curves in Figure 6 that when vibration frequency is equal to 30,000 Hz, the average velocities of particles are almost same, which indicate that it is unnecessary for high vibration frequency to choose high feed rate of workpiece.

Figure 4 The *X*-direction velocity of abrasive grains, (a) 7,000 Hz (b) 10,000 Hz (c) 20,000 Hz (d) 30,000 Hz

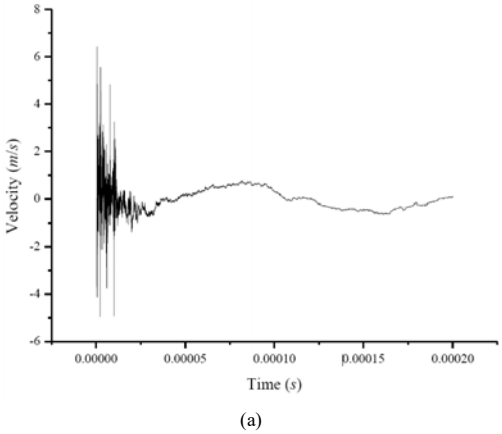

(a)

Figure 4 The *X*-direction velocity of abrasive grains, (a) 7,000 Hz (b) 10,000 Hz (c) 20,000 Hz (d) 30,000 Hz (continued)

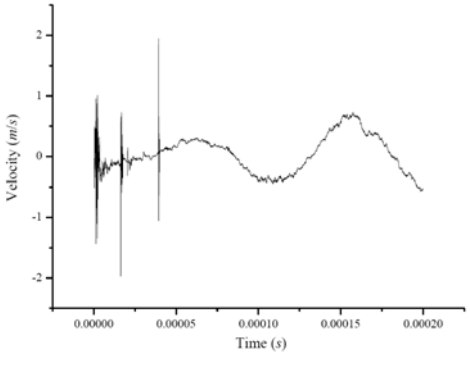

(b)

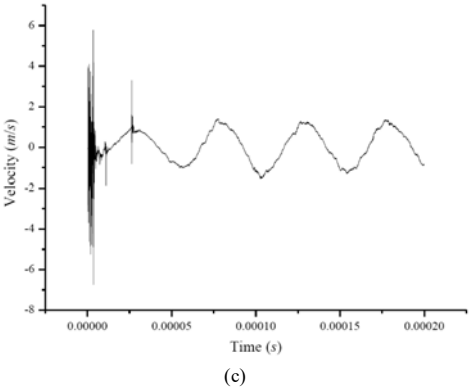

(c)

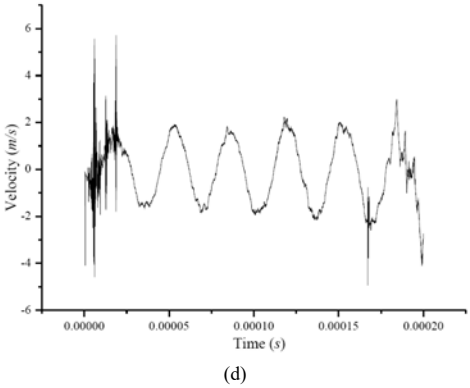

(d)

Figure 5 The motion velocity of abrasive grains, (a) 7,000 Hz (b) 10,000 Hz (c) 20,000 Hz (d) 30,000 Hz (see online version for colours)

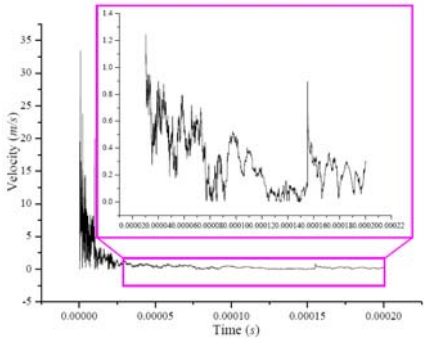

(a)

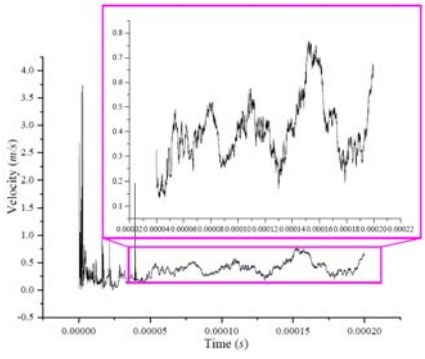

(b)

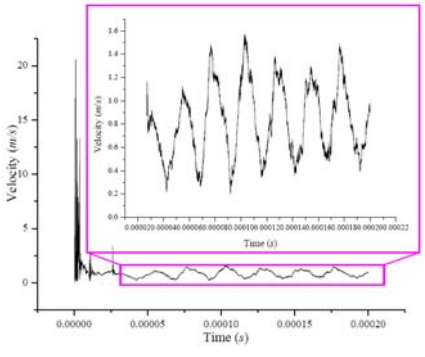

(c)

Figure 5 The motion velocity of abrasive grains, (a) 7,000 Hz (b) 10,000 Hz (c) 20,000 Hz (d) 30,000 Hz (continued) (see online version for colours)

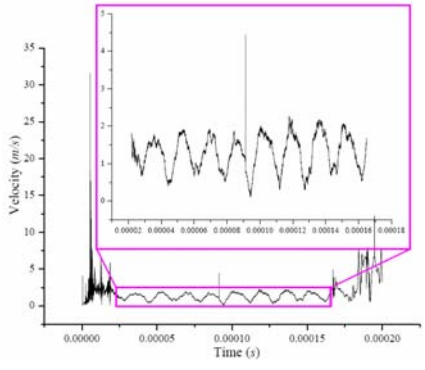

(d)

Figure 6 The changes of average velocity at different frequencies (see online version for colours)

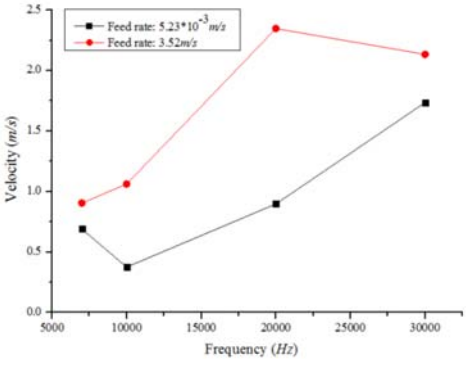

3.1.2 The effects of vibration amplitude on the particle velocity

Figure 7 shows that average velocity changes of particles at different vibration amplitudes (feed rate: 5.23 * 10^{-3} m/s, frequency: 20,000 Hz, polishing force: 30 mN). Vibration amplitudes: 1 μm, 5 μm, 10 μm, 20 μm, 30 μm and 40 μm. The change of velocity is given in Figure 7(a) for amplitude 1 μm and it can be seen that it is irregular with increase of time. So vibration amplitude should not be too small. Figures 7(b), 7(c) and 7(d) show that the changes of particles velocity are very rapid at the beginning of polishing and the particles velocities go into a stable stage after 5.0 * 10^{-5} s. In addition,

Figures 7(b), 7(c) and 7(d) also show the motion velocity of abrasive grains after going into the stable stage. It can be seen from these three figures that the velocity curves of 10 μm, 20 μm and 40 μm are similar to the sinusoidal curves, there are good relations between the velocity variation period and vibration period, and especially the maximum velocity also increases with increase of vibration amplitude. Figure 8 is average velocity changes of particles versus vibration amplitude. As shown Figure 8, when other parameters keep constants, average motion speed of the abrasive particles increase approximately linearly with increase of vibration amplitude, which indicates increasing vibration amplitude can also increase properly polishing efficiency in practice.

Figure 7 The changes of velocity at different amplitudes, (a) 1 μm (b) 10 μm (c) 20 μm (d) 40 μm (see online version for colours)

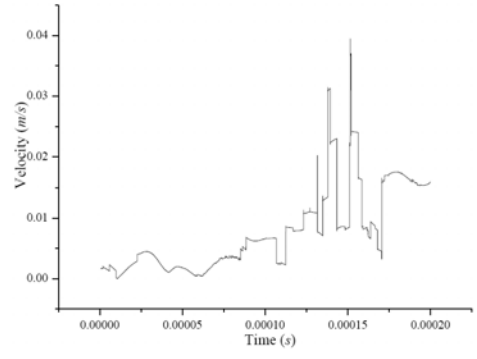

(a)

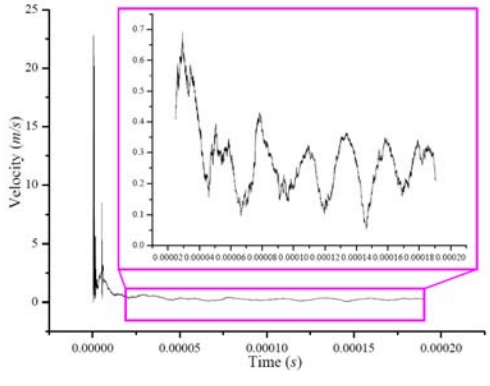

(b)

Figure 7 The changes of velocity at different amplitudes, (a) 1 μm (b) 10 μm (c) 20 μm (d) 40 μm (continued) (see online version for colours)

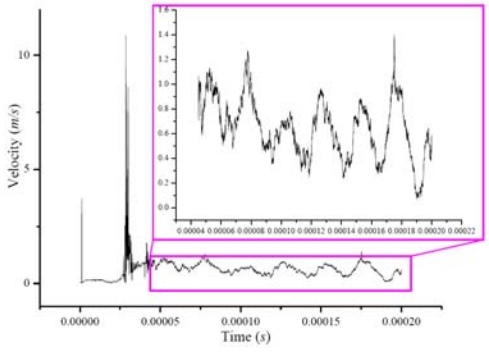

(c)

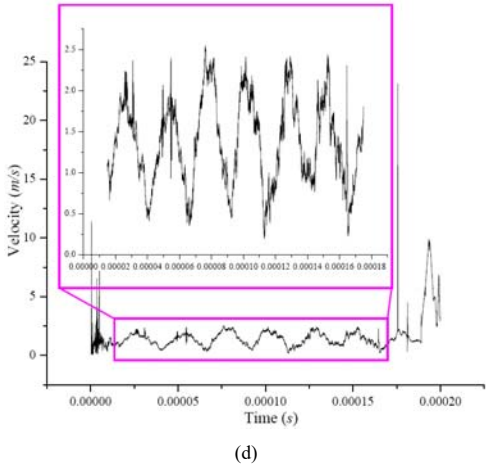

(d)

Figure 8 The particles average velocity for different vibration amplitudes (see online version for colours)

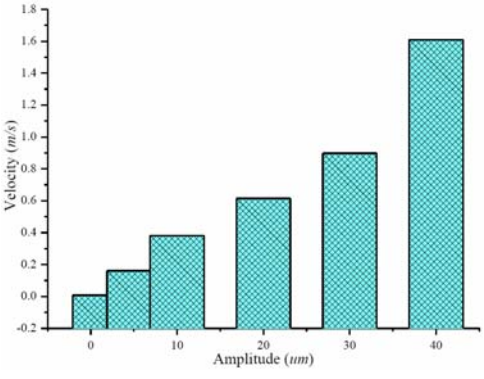

3.2 The effects of vibration on the unbalanced force

3.2.1 The effects of vibration frequencies on the unbalanced force

It is all known that the force acting on the workpiece surface is an important process parameter that has effects on material removal rate, surface quality and maching efficiency. In the simulation model, the polishing force applying to the workpiece surface by the tool is equal to 30 mN throughout, however, the force on the workpiece surface is constantly changing, which is always subject to variation when changing the vibration parameters. This dynamic force is defined as the unbalanced force in this study, which is refer to a comprehensive force acting on the workpiece containing the force provided by the fluid flowing, abrasive grains moving, vibrating of polishing tool, and the force applying actively by the tool. During PFC^{3D} simulations, these unbalanced forces in *X*- *Y*- and *Z*-direction were recorded respectively at every moment, and then the magnitude of the resultant force at every moment was calculated. Figure 9 shows the changes of unbalanced force at different vibration frequencies. Figure 10 shows that the unbalanced force varies with the vibration frequencies for various feed rates.

It can be seen from Figure 9 that the unbalanced force acting on the workpiece changes rapidly at the begin of polishing, going into a stable stage after 2.5 * 10^{-4} s, which is equal to that of the particles going into stable stage approximately, all the change curves are similar to the triangular wave curves. Although the workpiece was applied a force (30 mN) by the polishing tool in the model, it can be seen from Figure 9 that the unbalanced forces at initial stage are more than 30 mN, the unbalanced forces of entering the stage are basically less than 30 mN, and all the maximum forces under different vibration frequencies are about 30 mN. So it can be concluded that, by the polishing tool's vibration, increasing of abrasive grains' average motion velocity also

make the unbalanced force change accordingly. It can be seen from Figure 10 that the unbalanced force increases on the whole with increase of vibration frequency when feed rate is 5.23 * 10^{-3} m/s, which indicates that the influence of vibration frequencies on the unbalanced force is evidently in low feed rate. It also can be seen from Figure 10 that the unbalanced force doesn't increase linearly with the increase of vibration frequency when feed rate is relatively high (3.52 m/s), and there is a drastic increase in the unbalanced force (about 65 mN) when the vibration frequency is 2,000 Hz. It may be that there are excessive unbalanced forces in the initial instability stage, or there are also excessive unbalanced forces in a transient calculation after entering the stable stage. In addition, Figure 10 shows that all the average forces are not equal to 30 mN, which indicates that the unbalanced forces acting on the workpiece surface will change due to the polishing tool' vibration and the abrasive grains' cutting. According to the Preston equation, the material removal rate is directly proportional to the polishing force. So, it can be concluded that high frequency vibration can significantly improve polishing efficiency, especially when feed rate is low.

Figure 9 The changes of unbalanced force with low feed rate (5.23 * 10^{-3} m/s), (a) 7,000 Hz (b) 10,000 Hz (c) 200,000 Hz (see online version for colours)

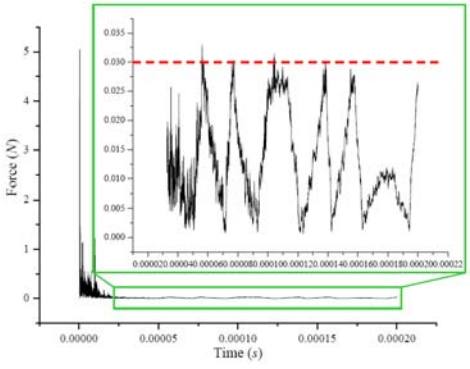

(a)

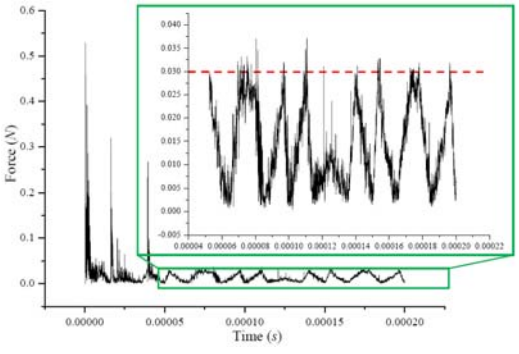

(b)

Figure 9 The changes of unbalanced force with low feed rate (5.23 * 10^{-3} m/s), (a) 7,000 Hz (b) 10,000 Hz (c) 200,000 Hz (continued) (see online version for colours)

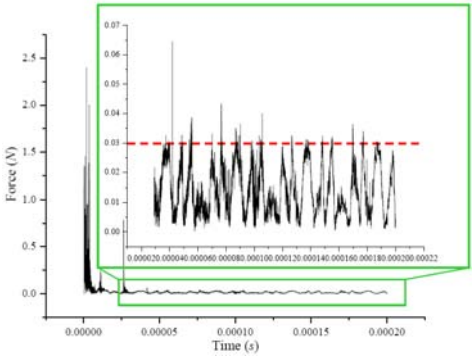

(c)

Figure 10 The changes of average force for different frequencies (see online version for colours)

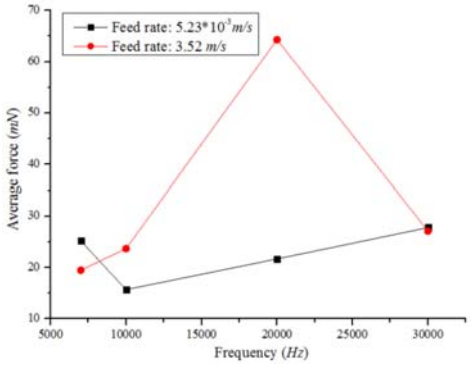

3.2.2 The effects of vibration amplitude on the unbalanced force

Figure 11 shows that the changes of unbalanced force at different vibration amplitudes (feed rate: 5.23 * 10^{-3} m/s, frequency: 20,000 Hz, polishing force: 30 mN). Vibration amplitudes are 1 μm, 10 μm, 20 μm and 40 μm respectively. Figure 12 is the average the unbalanced force versus the vibration amplitude. Figures 11(b), 11(c) and 11(d) show that the unbalanced forces change very rapidly at the beginning of polishing and go into a stable stage after 5.0 * 10^{-5} s. The unbalanced forces for the amplitudes 1 μm and 10 μm given in Figures 11(a) and 11(b) have regularly fluctuation after entering the stage. The change curves for the amplitudes 20 μm and 40 μm are similar to the triangular wave curves. It can be seen from Figures 11(b), 11(c) and 11(d) that the unbalanced forces at initial stage are more than 30 mN, the unbalanced forces of entering the stage is basically

less than 30 mN, and all the maximum forces that are about 30 mN under different vibration amplitudes have an increasing trend with the increase of vibration amplitude. Figure 11 can also shows that the cycle of unbalanced force decreases with the increase of vibration amplitude. Figure 12 clearly shows that, when other parameters keep constants, the unbalanced force increases approximately linearly with increase of vibration amplitude, which indicates the polishing efficiency can be improve by increasing of vibration amplitude properly.

Figure 11 The changes of unbalanced force for different vibration amplitudes, (a) 1 μm (b) 10 μm (c) 20 μm (d) 40 μm (see online version for colours)

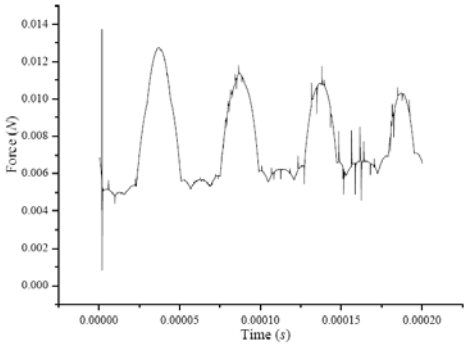

(a)

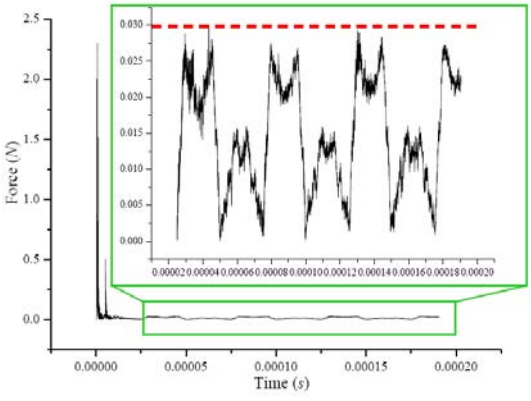

(b)

Figure 11 The changes of unbalanced force for different vibration amplitudes, (a) 1 μm (b) 10 μm (c) 20 μm (d) 40 μm (continued) (see online version for colours)

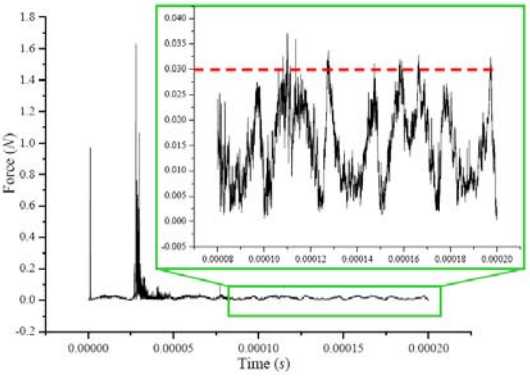

(c)

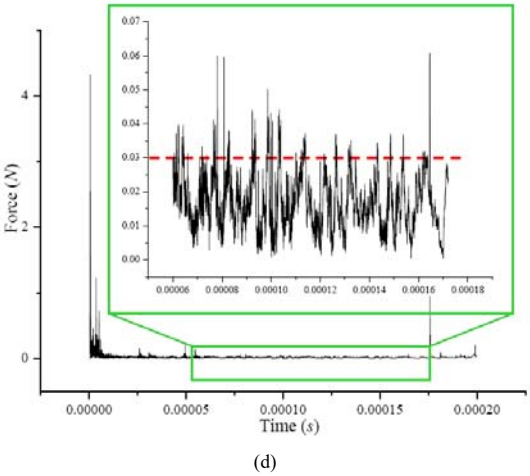

(d)

Figure 12 The changes of average unbalanced force for different vibration amplitudes (see online version for colours)

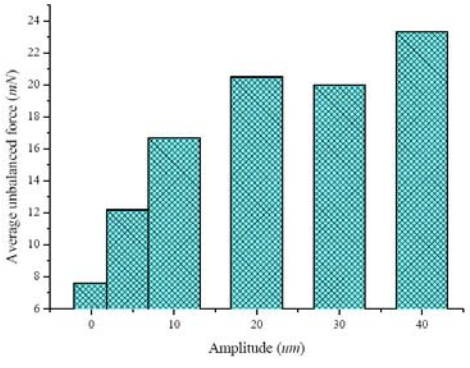

At last, it could be concluded from above analyses in this study that, with increase of vibration frequency and amplitude, the interaction result of motion velocity of abrasive grains and the average unbalanced force can improve polishing efficiency and surface roughness on the whole, which is the same as the laws obtained from other experiment results in reference (Zhao et al., 2016).

4 Conclusions

A model for vibration assisted mechanical polishing micro-structured surface based on PFC^{3D} was presented using DEM. The effects of vibration on polishing process were analysed in detail under micro-scale. Unbalanced force is introduced to quantise comprehensive effects of the tool, liquid and abrasive grains on the micro-structured surface. The simulation results show the obvious differences in fluid pressure, abrasive grains velocity and unbalanced force with the changes in vibration frequency and amplitude. The following results were obtained:

1 The effect laws of vibration on the motion velocity of abrasive grains are firstly given in this study. Average velocity of abrasive grains increases with increase of vibration frequency, and all the change curves of velocity are similar to the sinusoidal curves and the feature similar to the sinusoidal curves is more obvious with increase of vibration frequency. Especially when the workpiece feed rate is low, a higher vibration frequency should be chosen. Average velocity of abrasive grains increase approximately linearly with increase of vibration amplitude. The simulation results show that high frequency vibration makes abrasive grains move more actively. It is concluded that the main effect of vibration in polishing process can increase the relative velocity between the workpiece and abrasive grains.

2 The effect laws of vibration on the unbalanced force were researched. It can be found that frequency and amplitude have important effects on the unbalanced force acting on the workpiece surface. When the feed rate is relatively low, after going into stable

stage with different frequencies and amplitude, the change curves similar to the wave curves with the periodicity, the unbalanced force is basically less than the force initially applying to the workpiece by the tool, and all the maximum unbalanced forces are about this force. The changes of average unbalanced force evidently increase with the increase of vibration frequency. The unbalanced force fluctuates obviously under high vibration frequency. On the whole, the average unbalanced force increases approximately linearly with the increase of vibration amplitude. Based on comprehensive analysis, it is concluded that vibration with high frequency and great amplitude can significantly increase material removal rate and improve surface quality in the polishing process of micro-structured surface.

Acknowledgements

This work was supported by the National Natural Science Foundation of China (51405196), the Natural Science Foundation of Tianjin (18JCYBJC20100, 17JCZDJC30400), and Tianjin application foundation and advanced technology research programme (the youth fund project) (Grant No. 17JCQNJC01700).

References

Agrawal, P.M., Raff, L.M., Bukkapatnam S. and Komanduri, R. (2010) 'Molecular dynamics investigations on polishing of a silicon wafer with a diamond abrasive', *Applied Physics A*, Vol. 100, No. 1, pp.89–104.

Ancio, F., Gámez, A.J. and Marcos, M. (2018) 'Superficial alterations in the generation of a 3D surface. The case of machining by turning. Application of principal component analysis to the study of the various factors involved', *International Journal of Surface Science & Engineering*, Vol. 12, No. 2, pp.77–98.

André, D., Charles, J.L., Iordanoff, I. and Néauport, J. (2014) 'The GranOO workbench, a new tool for developing discrete element simulations, and its application to tribological problems', *Advances in Engineering Software*, Vol. 74, pp.40–48.

André, D., Iordanoff, I., Charles, J.L. and Néauport, J. (2012) 'Discrete element method to simulate continuous material by using the cohesive beam model', *Computer Methods in Applied Mechanics and Engineering*, Vols. 213–216, pp.113–125.

André, D., Jebahi, M., Iordanoff, I., Charles, J.L. and Néauport, J. (2013) 'Using the discrete element method to simulate brittle fracture in the indentation of a silica glass with a blunt indenter', *Computer Methods in Applied Mechanics and Engineering*, Vol. 265, pp.136–147.

Belkhir, N., Aliouane, T. and Bouzid, D. (2014) 'Correlation between contact surface and friction during the optical glass polishing', *Applied Surface Science*, Vol. 288, pp.208–214.

Blaineau, P., André, D., Laheurte, R., Darnis, P., Darbois, N., Cahuc, O. and Neauport, J. (2015) 'Subsurface mechanical damage during bound abrasive grinding of fused silica glass', *Applied Surface Science*, Vol. 353, pp.764–773.

Cao, Z.C., Cheung, C.F. and Zhao, X. (2016) 'A theoretical and experimental investigation of material removal characteristics and surface generation in bonnet polishing', *Wear*, Vols. 360–361, pp.137–146.

Eder, S.J., Cihak-Bayr, U. and Pauschitz, A. (2015) 'Nanotribological simulations of multi-grit polishing and grinding', *Wear*, Vols. 340–341, pp.25–30.

Fan, Q.T., Zhu, J.Q., Zhang, B.A. and Bao, L. (2007) 'Motion simulation of annular polishing', *International Journal of Computer Applications in Technology*, Vol. 29, Nos. 2–4, pp.159–162.

Fillot, N., Iordanoff, I. and Berthier, Y. (2007) 'Modelling third body flows with a discrete element method – a tool for understanding wear with adhesive particles', *Tribology International*, Vol. 40, No. 6, pp.973–981.

Guo, J. and Suzuki, H. (2018) 'Effects of process parameters on material removal in vibration-assisted polishing of micro-optic mold', *Micromachines*, Vol. 9, No. 7, 349.

Guo, J., Mortia, S.Y., Hara, M., Yamagata, Y. and Higuchi, T. (2012) 'Ultra-precision finishing of micro-aspheric mold using a magnetostrictive vibrating polisher', *International Journal of Machine Tools & Manufacture*, Vol. 61, No. 1, pp.371–374.

Guo, J., Suzuki, H. and Higuchi, T. (2013) 'Development of micro polishing system using a magnetostrictive vibrating polisher', *Precision Engineering*, Vol. 37, No. 1, pp.81–87.

Han, L., Zhao, H.W., Zhang, Q.X., Jin, M.J., Zhang, L. and Zhang, P. (2015) 'Research on influences of contact force in chemical mechanical polishing (CMP) process', *AIP Advances*, Vol. 5, No. 4, 041305, doi: 10.1063/1.4903700.

Han, X.S. (2014) 'Investigation of the surface generation mechanism of mechanical polishing engineering ceramics using discrete element method', *Applied Physics A*, Vol. 116, No. 4, pp.1729–1739.

Han, X.S. and Gan, Y.X. (2011) 'Analysis the complex interaction among flexible nanoparticles and materials surface in the mechanical polishing process', *Applied Surface Science*, Vol. 257, No. 8, pp.3363–3373.

Hreha, P. and Hloch, S. (2013) 'Potential use of vibration for metrology and detection of surface topography created by abrasive waterjet', *International Journal of Surface Science & Engineering*, Vol. 7, No. 2, pp.135–151.

Huuki, J. and Laakso, S.V.A. (2017) 'Surface improvement of shafts by the diamond burnishing and ultrasonic burnishing techniques', *International Journal of Machining and Machinability of Material*, Vol. 19, No. 3, pp.246–259.

Iliescu, D., Gehin, D., Iordanoff, I., Girot, F. and Gutiérrez, M.E. (2010) 'A discrete element method for the simulation of CFRP cutting', *Composites Science and Technology*, Vol. 70, No. 1, pp.73–80.

Iordanoff, I., Battentier, A., Néauport, J. and Charles, J.L. (2008) 'A discrete element model to investigate sub-surface damage due to surface polishing', *Tribology International*, Vol. 41, No. 11, pp.957–964.

Jerier, J.F. and Molinari, J.F. (2012) 'Normal contact between rough surfaces by the discrete element method', *Tribology International*, Vol. 47, pp.1–8.

Jiang, S.Q., Li, T.T. and Tan, Y.Q. (2015) 'A DEM methodology for simulating the grinding process of SiC ceramics', *Procedia Engineering*, Vol. 102, pp.1803–1810.

Li, C.H., Liu, Z.R., Hou, Y.L. and Ding, Y.C. (2012) 'Analytical and experimental investigations into material removal mechanism of abrasive jet precision finishing with grinding wheel as restraint', *International Journal of Machining and Machinability of Materials*, Vol. 12, No. 3, pp.266–279.

Li, L., He, Q., Zheng, M., Ren, Y. and Li, X.L. (2019) 'Improvement in polishing effect of silicon wafer due to low-amplitude megasonic vibration assisting chemical-mechanical polishing', *Journal of Materials Processing Technology*, Vol. 263, No. 3, pp.330–335.

Li, Y.G., Wu, Y.B., Zhou, L.B. and Fujimoto, M. (2014a) 'Vibration-assisted dry polishing of fused silica using a fixed-abrasive polisher', *International Journal of Machine Tools & Manufacture*, Vol. 77, pp.93–102.

Li, Z., You, M., Wang, J., Li, G.Y. and Li, D.M. (2014b) 'Numerical simulation of influence factors of stress distribution of weld-bonded joint under peeling load', *International Journal of Computer Applications in Technology*, Vol. 50, Nos. 3–4, pp.232–237.

Liang, C.L., Liu, W.L., Zheng, Y.H., Ji, X.L., Li, S.S., Yin, W.J., Guo, X.H. and Song, Z.T. (2016) 'Fractal nature of non-spherical silica particles via facile synthesis for the abrasive particles in chemical mechanical polishing', *Colloids and Surfaces A: Physicochemical and Engineering Aspects*, Vol. 500, pp.146–153.

Liedke, T. and Kuna, M. (2013) 'Discrete element simulation of micromechanical removal processes during wire sawing', *Wear*, Vol. 304, Nos. 1–2, pp.77–82.

Lin, Y.Y., Lo, S.P. and Chen, C.Y. (2006) 'Strain and stress analysis of the oxide film surface in the chemical mechanical polishing process', *International Journal of Computer Applications in Technology*, Vol. 26, No. 4, pp.233–241.

Loresch, I. and Riemer, O. (2015) 'Modelling of grain motion for three-body abrasion', *Procedia CIRP*, Vol. 31, pp.282–286.

Maroju, N.K., Krishna, P.V. and Jin, X.L. (2017) 'Assessment of high and low frequency vibration assisted turning with material hardness', *International Journal of Machining and Machinability of Materials*, Vol. 19, No. 2, pp.110–135.

Mullany, B. and Mainuddin, M. (2012) 'The influence of process vibrations on precision polishing metrics', *CIRP Annals-Manufacturing Technology*, Vol. 61, No. 1, pp.555–558.

Salvatore, F., Mabrouki, T. and Hamdi, H. (2017) 'Analytical modelling of material removal process in the case of orthogonal cutting and worn tools', *International Journal of Machining and Machinability of Material*, Vol. 19, No. 6, pp.570–586.

Song, D.L., Zhao, J., Ji, S.J and Zhou, X.Q. (2016) 'Development of a novel two-dimensional ultrasonically actuated polishing process', *AIP Advances*, Vol. 6, No. 11, 115105, doi: 10.1063/1.4967292.

Sun, J.P., Fang, L., Han, J., Han, Y., Chen, H.W. and Sun, K. (2014) 'Phase transformations of mono-crystal silicon induced by two-body and three-body abrasion in nanoscale', *Computational Materials Science*, Vol. 82, pp.140–150.

Suzuki, H., Hamada, S., Okino, T., Kondo, M., Yamagata, Y. and Higuchi, T. (2010) 'Ultraprecision finishing of micro-aspheric surface by ultrasonic two-axis vibration assisted polishing', *CIRP Annals – Manufacturing Technology*, Vol. 59, No. 1, pp.347–350.

Suzuki, H., Moriwaki, T., Okino, T. and Ando, Y. (2006) 'Development of ultrasonic vibration assisted polishing machine for micro aspheric die and mold', *Annals of the CIRP*, Vol. 55, No. 1, pp.385–388.

Tan, Y.Q., Yang, D.M. and Sheng, Y. (2009) 'Discrete element method (DEM) modeling of fracture and damage in the machining process of polycrystalline SiC', *Journal of the European Ceramic Society*, Vol. 29, No. 6, pp.1029–1037.

Uhlmann, E., Dethlefs, A. and Eulitz, A. (2014) 'Investigation of material removal and surface topography formation in vibratory finishing', *Procedia CIRP*, Vol. 14, pp.25–30.

Uhlmann, E., Eulitz, A. and Dethlefs, A. (2015) 'Discrete element modelling of drag finishing', *Procedia CIRP*, Vol. 31, pp.369–374.

Wang, Y., Fu, Z., Dong, Y., Liu, S. and Lu, S. (2018) 'Research on surface generating model in ultrasonic vibration-assisted grinding', *International Journal of Advanced Manufacturing Technology*, Vol. 96, Nos. 9–12, pp.1–8.

Xiu, S.C., Cai, G.Q. and Li, C.H. (2007) 'Study on surface finish mechanism in quick-point grinding', *International Journal of Computer Applications in Technology*, Vol. 29, Nos. 2–4, pp.163–167.

Xu, W.H., Lu, X.C., Pan, G.S., Lei, Y.Z. and Luo, J.B. (2011) 'Effects of the ultrasonic flexural vibration on the interaction between the abrasive particles; pad and sapphire substrate during chemical mechanical polishing (CMP)', *Applied Surface Science*, Vol. 257, No. 7, pp.2905–2911.

Yang, N., Zong, W.J., Li, Z.Q. and Sun, T. (2015) 'Wear process of single crystal diamond affected by sliding velocity and contact pressure in mechanical polishing', *Diamond & Related Materials*, Vol. 58, pp.46–53.

Yu, T.B., An, J.H., Yang, X.Z., Bian, X.S. and Zhao, J. (2018) 'The study of ultrasonic vibration assisted polishing optical glass lens with ultrasonic atomizing liquid', *Journal of Manufacturing Processing*, Vol. 34, pp.389–400.

Zhao, Q.L., Sun, Z.Y. and Guo, B. (2016) 'Material removal mechanism in ultrasonic vibration assisted polishing of micro cylindrical surface on SiC', *International Journal of Machine Tools & Manufacture*, Vol. 103, pp.28–39.

Zhu, A.B., He, D.Y., Luo, W.C. and Liu, Y.Y. (2016) 'Role of crystal orientation on chemical mechanical polishing of single crystal copper', *Applied Surface Science*, Vol. 386, pp.262–268.